

Mesoscopic Spin-Boson Models of Trapped Ions

D. Porras¹, F. Marquardt², J. von Delft², and J. I. Cirac¹

¹ *Max-Planck Institut für Quantenoptik, Hans-Kopfermann-Str. 1, Garching, D-85748, Germany.*

² *Physics Department, Arnold Sommerfeld Center for Theoretical Physics, and Center for NanoScience, Ludwig-Maximilians-Universität München, 80333 München, Germany.*

(Dated: October 22, 2021)

Trapped ions arranged in Coulomb crystals provide us with the elements to study the physics of a single spin coupled to a boson bath. In this work we show that optical forces allow us to realize a variety of spin-boson models, depending on the crystal geometry and the laser configuration. We study in detail the Ohmic case, which can be implemented by illuminating a single ion with a travelling wave. The mesoscopic character of the phonon bath in trapped ions induces new effects like the appearance of quantum revivals in the spin evolution.

PACS numbers: PACS

The problem posed by a two-level system interacting with a bath of harmonic oscillators, known as the spin-boson model, appears in condensed matter, atomic physics, and quantum information processing. It is of fundamental importance, since it represents a paradigm for the study of quantum dissipation and the quantum-to-classical transition [1, 2, 3]. The spin-boson model displays nonperturbative features of many-body physics, like the localization transition at a critical dissipation strength. For the special case of an Ohmic bath spectrum, it may be mapped onto the celebrated Kondo Hamiltonian. Despite its fundamental importance, experimental investigations into anything but the weak-coupling regime of the spin-boson model are still scarce. The localization transition has been observed in the related Josephson junction systems [4], while typical solid-state two-level systems feature a coupling strength much below the critical threshold [5].

Trapped ions provide a clean experimental model system which is ideally suited for the quantum simulation of condensed matter problems [6, 7]. As we show in this work, the spin-boson model appears here in a natural way, with a wide range of tunable parameters. The role of the two-level system is played by two internal levels of a single ion that is part of a Coulomb crystal. Since ions interact through the Coulomb repulsion, their motion is described by collective modes with a dispersion relation which depends both on the direction of vibration and on the trapping conditions. The internal level of the single ion can be coupled to the vibrational bath by means of optical forces [8], in such a way that several different spin-boson couplings may be implemented. Trapped ions offer us a wide range of possibilities for observing the phenomenology of the spin-boson model, with the advantage that we can use well-developed experimental techniques for the preparation of both the initial spin and phonon bath states [9]. Besides that, the finite number of vibrational modes forms a mesoscopic environment. This allows us to study memory effects due to the finite size of the system, such as quantum revivals in the spin

evolution, which are absent in the customary limit of a macroscopic bath.

In this work we analyze the spin-boson models which appear in systems of trapped ions, and we show the following results: (i) 1D and 2D Coulomb crystals provide us with a variety of phonon spectral densities, ranging from sub- to super-Ohmic, depending on the ion crystal dimension and the laser configuration. (ii) The particular case in which the internal level of a single ion is coupled to a Coulomb chain by a travelling wave corresponds to the Ohmic spin-boson model. If the number of ions is large enough, this setup allows us to tune the interaction strength and recover the standard phenomenology of this model, such as the quantum phase transition towards localization at strong coupling. (iii) For time scales larger than a given revival time, finite size effects induce the reexcitation of the spin after an initial period of relaxation (quantum revival), which can be observed in a wide range of parameters, including high temperatures of the phonon bath.

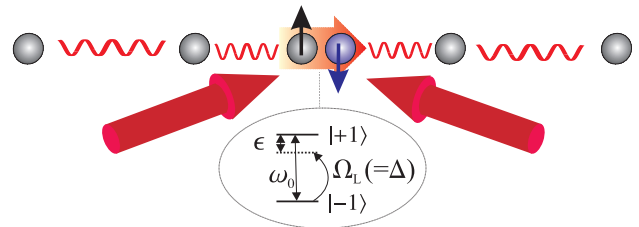


FIG. 1: (color online). Scheme of the implementation of spin-boson models in a Coulomb chain.

Experimental realization.—The standard spin-boson Hamiltonian is defined by

$$H = \frac{\epsilon}{2}\sigma_z + \frac{\Delta}{2}\sigma_x + \sum_n \left(\omega_n a_n^\dagger a_n + \frac{\sigma_z}{2} \lambda_n (a_n^\dagger + a_n) \right). \quad (1)$$

σ_α are the Pauli matrices, and ω_n and a_n are the energies and annihilation operators of the bath phonons,

respectively (we set $\hbar \equiv 1$). Two hyperfine levels $|-1\rangle$ and $|1\rangle$, separated by the internal energy ω_0 , correspond to the eigenstates of σ_z . We propose to experimentally realize the Hamiltonian (1) by addressing a single ion in a Coulomb crystal in one of two laser configurations (see Fig. 1): (i) *State dependent dipole force*. In this setup, a laser induces the tunneling term in Eq. (1), in such a way that the tunneling amplitude Δ and the bias ϵ are set by the laser's Rabi frequency, Ω_L , and the detuning, $\omega_0 - \omega_L$, respectively. The spin-phonon coupling is induced by subjecting the selected ion to an off-resonant standing wave, which creates the state dependent dipole potential $V(z) = V_0 \cos^2(kz + \phi) \sigma_z$. k and ϕ are the wavevector and phase of the standing wave lasers, respectively. The operator z is the ion's coordinate in the direction of the optical force relative to its equilibrium position. It is readily expressed in terms of phonon operators, $z = \sum_n \mathcal{M}_n \bar{z}_n (a_n + a_n^\dagger)$, where $\bar{z}_n = 1/\sqrt{2m\omega_n}$, with m the ion mass, and \mathcal{M}_n is the amplitude of each vibrational mode n at the ion. In the Lamb-Dicke regime ($kz \ll 1$) we can expand $V(z)$,

$$H_{\text{sw}} = \frac{1}{2} \sigma_z (V(0) + Fz + Qz^2). \quad (2)$$

$V(0)$ is just a shift of the bias ϵ , and by choosing ϕ appropriately one can retain the linear or the quadratic terms in (2) only. We focus on the case of a linear coupling ($\phi = \pi/4$, $Q = 0$), which leads to (1) with $\lambda_n^{\text{sw}} = F\mathcal{M}_n \bar{z}_n$. (ii) *Polaron coupling induced by a travelling wave*. In this setup a single laser creates both the spin-boson coupling and the tunneling term in Eq. (1). One of the trapped ions in the chain interacts with a travelling wave, such that the coupling is given, in a frame rotating with ω_L , by

$$H_{\text{tw}} = \frac{\Omega_L}{2} (\sigma^\dagger e^{ikz} + \sigma^- e^{-ikz}). \quad (3)$$

Hamiltonian (3) can be recast to fit the expression (1) by applying the canonical transformation $U = e^{-(i/2)kz\sigma^z}$, which yields $\lambda_n^{\text{tw}} = k\bar{z}_n \mathcal{M}_n \omega_n$, $\Delta = \Omega_L$, and $\epsilon = \omega_0 - \omega_L$.

Spectral density.—The properties of the spin-boson model are determined by the spectral density, $J(\omega) = \pi \sum_{n=1}^N \lambda_n^2 \delta(\omega - \omega_n)$. The model shows a rich phenomenology that has mostly been analyzed for the case of an infinite gapless bath, such that $J(\omega) \propto \omega^s$. In this work we focus on describing experimental conditions that lead to this situation. Two main cases are relevant, namely, 1D and 2D Coulomb crystals. Although finite size effects will play an important role, and will be discussed below, we will first revisit the thermodynamical limit, $N \rightarrow \infty$, to understand some of the main features. The axial (1D) or in-plane (2D) modes can be considered approximately gapless, since the minimum energy is the global trapping frequency along the crystal, which has to be small enough to guarantee the stability of the latter. For a 1D Coulomb chain of ions

with equally spaced equilibrium positions, the low energy spectrum of axial vibrations [10] is approximately given by $\omega_n^{1D} = v\omega_z \frac{\pi n}{N} (1 - \frac{2}{3} \log(\frac{\pi n}{N}))^{1/2}$, where $v = \sqrt{3\beta/2}$, ω_z is the axial trapping frequency, and $\beta = 2e^2/(m\omega_z^2 d_0^3)$, with d_0 the mean distance. In order to get a qualitative description, we will retain the linear term only (see Fig. 2 (a)), and get the following spectral densities for each coupling:

$$J_{\text{sw}}^{1D}(\omega) = (1/v)\bar{\mathcal{M}}^2 (Fz_0)^2 \omega^{-1}, \quad (4)$$

$$J_{\text{tw}}^{1D}(\omega) = (1/v)\bar{\mathcal{M}}^2 \eta^2 \omega = 2\pi\alpha \omega, \quad (5)$$

where $\bar{\mathcal{M}}$ is the mode function of axial phonons at the addressed ion, $\eta = k/\sqrt{2m\omega_z}$ is the Lamb-Dicke parameter, and we have reexpressed $J_{\text{tw}}^{1D}(\omega)$ as a function of the dimensionless dissipation strength α [1]. Finite size effects will modify the spectral density of a Coulomb crystal. Nevertheless, Eqs. (4) and (5) allow us to determine the character of the phonon bath, as well as the scaling of its properties with experimental parameters. This is shown by the comparison with exact numerical calculations in Fig. 2. Finally, in a 2D Coulomb crystal, ions arrange themselves in a triangular lattice [11]. There, the lowest energy vibrational modes also show a linear dispersion relation [12], such that the corresponding spin-boson models have an algebraic spectral density with exponents $s = 0$ [13] and $s = 2$, in the cases of interaction with a standing wave, or a travelling wave, respectively.

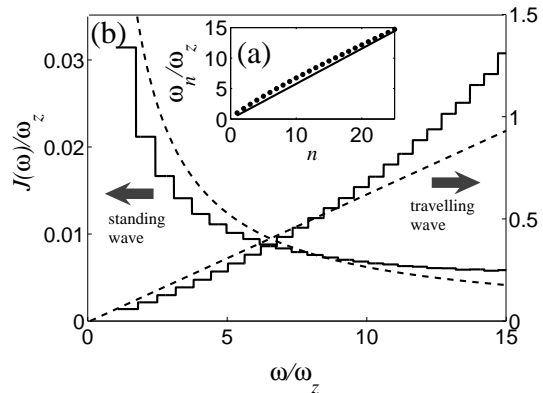


FIG. 2: Phonon bath properties of a Coulomb chain with $N = 50$ ions. (a) Dots: Axial vibrational spectrum. Continuous line: Approximation given by retaining the linear terms in ω_n^{1D} . (b) Spectral density corresponding to spin-boson couplings induced by a standing or a travelling wave. The continuous lines are obtained with the exact vibrational spectrum, by substituting the delta function in $J(\omega)$ by a constant function in each interval (ω_n, ω_{n+1}) , of height $(\omega_{n+1} - \omega_n)^{-1}$. The dashed lines are the approximations of Eqs. (4) and (5).

Trapped ion Ohmic model.—In the following we analyze in detail the spin-boson model induced by a travelling wave interacting with the central ion of a Coulomb

chain, which leads to (5). Since this case corresponds to Ohmic dissipation, it shows a rich phase diagram as a function of the temperature, T , and α [14]. Assume that at $t < 0$ the coupling (5) is off, the phonon bath is in thermal equilibrium, and the internal state is prepared in $|1\rangle$ by using standard optical pumping techniques. We focus on the evolution of the system at time $t > 0$, upon suddenly switching on the laser. In particular we calculate $P(t) = \langle \sigma^z \rangle$, to determine the evolution of the spin under the effect of the tunneling Δ [1]. The theoretical description of this system can be addressed within the Non-Interacting Blip Approximation (NIBA), which consists of a non-Markovian evolution equation for $P(t)$:

$$\begin{aligned} \dot{P}(t) &= \int_0^t K(t-t')P(t')dt', \\ K(\tau) &= -\Delta^2 \text{Re}\langle e^{ikz(\tau)} e^{-ikz(0)} \rangle, \end{aligned} \quad (6)$$

where the average is evaluated assuming a thermal state in the bosonic bath. This expression can be obtained by neglecting spin-bath correlations in a perturbative expansion up to second order in the tunneling amplitude Δ [15]. It is well established that it describes correctly the two limits of weak and strong dissipation, as well as the high temperature limit.

The finite-size properties of the spin-boson model defined by Eq. (3) can be qualitatively understood by considering the approximation that vibrational energies are equally spaced by a given energy $\delta\omega$. Under this assumption the Kernel $K(\tau)$ defined by (6) is periodic, and can be written as $K(\tau) = \sum_n \bar{K}(\tau - \tau_n)$, $\tau_n = n\tau_{\text{rev}}$, where $\tau_{\text{rev}} = 2\pi/\delta\omega$ is the vibrational bath revival time. $\bar{K}(\tau)$ becomes equal to the Kernel of the continuous Ohmic model in the limit $\tau_{\text{rev}} \rightarrow 0$. At short times ($t \ll \tau_{\text{rev}}$) the spin evolution is governed by $\bar{K}(\tau)$, and it shows a similar behavior as in the case of the continuum spin-boson model. The periodic structure of $K(\tau)$ manifests itself at long times ($\tau \geq \tau_{\text{rev}}$) in the form of quantum revivals in $P(t)$. The spin-boson model of trapped ions satisfies the condition of equally-spaced vibrational energies only approximately. However one can define an average energy spacing $\bar{\delta\omega}$, which in the limit of large N can be estimated by $\bar{\delta\omega} \approx v\omega_z\pi/N$. Thus, in a real Coulomb chain we expect that $\tau_{\text{rev}} \approx 2\pi/\bar{\delta\omega}$ defines the time scale which separates the short-time regime in the evolution of $P(t)$ coinciding with the evolution for a continuous bath, and the long-time regime displaying the quantum revivals.

Numerical solution.—To verify this assumption, we obtain the numerical solution of $P(t)$ within the NIBA, using the exact vibrational modes of a real ion chain. In order to compare the results obtained in the case of a real Coulomb chain with those predicted by the ideal Ohmic spin-boson model, we fit the exact low-energy spectral density to the form given by (5), and from there we extract the dissipation strength α which describes the ion

vibrational bath. The NIBA can be justified for a discrete phonon bath as long as the decay time of $\bar{K}(\tau)$ is much smaller than τ_{rev} . At short times $t \ll \tau_{\text{rev}}$, the validity of the NIBA in the continuous case implies that the average in Eq. (6) can be calculated by factorizing the total density matrix into the spin and phonon reduced density matrices. Due to the periodic structure of $K(\tau)$, brought about by the discreteness of the vibrational bath, we conclude that $P(t)$ is related to the state of the system at times $t - n\tau_{\text{rev}}$. In the first revival ($t \approx \tau_{\text{rev}}$), $P(t)$ depends on the state of the system at short-times, where the spin-bath decoupling scheme, which leads to the NIBA, works. Thus, the first revival is well described within in the NIBA, and the argument can be easily extended to later revivals. We checked the NIBA for the finite-size bath vs. the Weisskopf-Wigner approximation at weak coupling, finding very good agreement. The numerical solution of the NIBA integro-differential equation is performed by means of the numerical method presented in [16]. We now discuss in detail the results for two different regimes, depending on the phonon temperature.

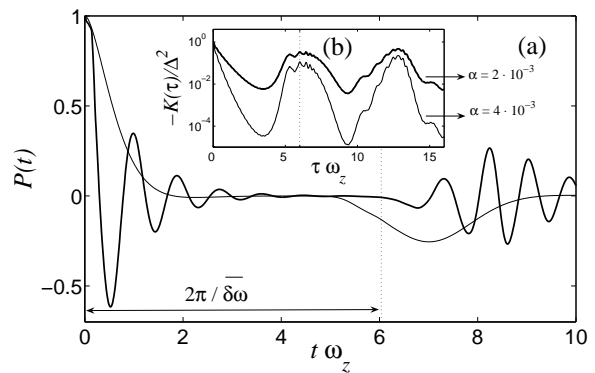


FIG. 3: (a) Transition from the underdamped (thick line, $\Delta = 10\omega_z$, $\alpha = 2 \cdot 10^{-3}$) to the overdamped regime (thin line, $\Delta = 3\omega_z$, $\alpha = 4 \cdot 10^{-3}$), in the high-temperature limit of a spin-boson model with $N = 50$ ions, $T = 250\omega_z$. (b) NIBA time kernels corresponding to these two regimes.

High temperature regime.—For sufficiently high temperatures, the kernel $\bar{K}(\tau)$ decays exponentially with a memory time $\tau_m = 1/(2\pi\alpha T)$ (we set $k_B = 1$). In the continuum limit one finds two main regimes: $\tau_m\Delta > 1$ (coherent oscillations) where $P(t)$ oscillates with Δ and decays in a time τ_m ; and $\tau_m\Delta < 1$ (overdamped relaxation) where $P(t)$ decays with a rate $\Gamma = \Delta^2\tau_m$. In the case of a finite Coulomb chain, $K(\tau)$ shows an exponential decay at short times, and additionally, an approximate periodic structure at time scales $\tau_{\text{rev}} \approx 2\pi/\bar{\delta\omega}$ (see Fig. 3 (b)). Fig. 3 (a) shows that the behavior of $P(t)$ at short times clearly reveals the transition between the overdamped and underdamped regimes, as well as the quantum revivals at τ_{rev} . The revival effect can be understood in terms of the perturbation of the Coulomb

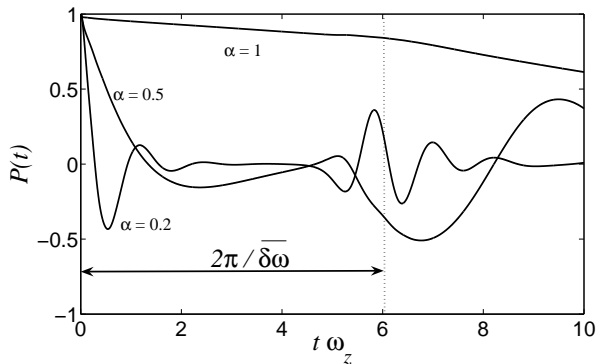


FIG. 4: Evolution of the spin population in the Ohmic trapped ion spin boson-model, in a Coulomb chain with $N = 50$ ions, $T = 0$, $\Delta = 10\omega_z$, and different dissipation strengths.

chain created during the initial spin relaxation, which propagates along the chain, is reflected at the boundaries, and returns to the selected ion, thus inducing its reexcitation. Interesting geometrical effects on the revivals may also be expected in $2D$ setups. Revivals in the high-temperature regime could be easily observed in experiments with trapped ions, since they require neither cooling to very low temperatures, nor high values of α .

Low temperature regime.—For the Ohmic model in the continuum and scaling limits, the evolution of $P(t)$ at $T = 0$ is determined by the value of α , in such a way that there are three regimes to be considered [1]: $\alpha < 1/2$ (coherent oscillations), $1/2 < \alpha < 1$ (overdamped relaxation), and $\alpha > 1$, in which case dissipation impedes the decay of $P(t)$ and the system becomes localized in the initial value of the effective spin [17]. Since the NIBA is known to reproduce the transition between these three regimes [18], we can use it to investigate whether the Ohmic spin-boson model in trapped ions shows the same transition. Our results are plotted in Fig. 4, where we show that the relaxation of $P(t)$ shows the same qualitative features as in the standard Ohmic model, with the appearance of quantum revivals at long times. The additional localization of the spin state is clearly evident at values of $\alpha > 1$, although a residual relaxation process still persists as a consequence of the discreteness of the bath. To quantify in more detail the transition to spin localization, we have calculated the initial decay rates at short times, as a function of α . Our results in Fig. 5(a) show the slowing down of the spin relaxation with increasing α , as well as the effect of finite temperatures. Note that Fig. 5(a) corresponds to the finite-size version of the quantum phase transition to localization which is found in the thermodynamical limit of the phonon bath (where Γ would vanish above $\alpha = 1$).

The strong dissipation regime of the mesoscopic Ohmic

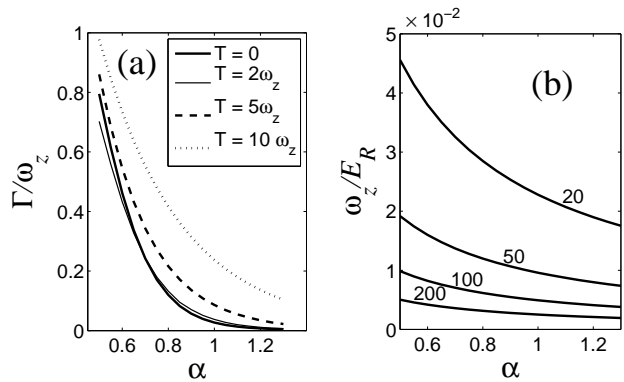


FIG. 5: (a) Evolution of the decay rate in the strong dissipation regime. $N = 50$, $\Delta = 10\omega_z$. (b) Axial trapping frequency of the trap that is required as a function of dissipation strength in units of the recoil energy, with different values of N . $E_R = k^2/2m$, with k the wavevector in (3). For example, Be^+ , $2\pi/k = 300$ nm, yields $E_R = 245$ kHz.

spin-boson model requires high values of α , and thus of $\eta^2 \propto 1/\omega_z$. In the case of a chain with $N = 50$ ions, the transition to localization can be observed with ω_z of a few kHz. The axial trapping frequency that is required to realize a model with a given α decreases with N , see Fig. 5(b). This condition is difficult to meet in an experiment, due to the need to cool the Coulomb chain to low temperatures. However, it must be noted that ground state cooling is not required. Our calculations show that up to temperatures of the order of the axial trapping frequency the transition to localization can still be observed, whereas at higher temperatures it is smeared out.

Outlook.—Let us comment on the possibility of implementing various interesting experimental situations other than the ones discussed above. In particular, the coupling (2) allows us to implement a bath with $1/f$ -noise, a model which is relevant to the description of decoherence of solid-state qubits (both normal and superconducting) [19]. Besides that, according to our discussion for the case of an off-resonant standing wave addressing the selected ion, it is possible to tune the spin-boson coupling in such a way that we implement spin-boson models with couplings quadratic in the bath coordinate. Again, these are of current concern in the description of superconducting solid-state qubits operating at the 'sweet spot' [20], and could be studied in much more detail in an ion chain model. Finally, the simultaneous coupling of several spins to the vibrational bath, by addressing several ions with lasers, would represent an implementation of a 'many spin-boson' model, where the interplay between the phonon bath-mediated spin-spin coupling and dissipation could be studied.

Work supported by EU projects (SCALA and CONQUEST), the DFG through SFB 631, NIM, and an Emmy-Noether grant (F.M.).

-
- [1] A. J. Leggett *et al.*, Rev. Mod. Phys. **59**, 1 - 85 (1987).
- [2] U. Weiss, *Quantum dissipative systems*, World Scientific, Singapore (1999).
- [3] See the special issue, Chem. Phys. **296**, 101 - 366 (2004), for recent views on the spin-boson model.
- [4] J.S. Pentillä *et al.*, Phys. Rev. Lett. **82**, 1004 (1999).
- [5] T. Hayashi *et al.*, Phys. Rev. Lett. **91**, 226804 (2003).
- [6] D. Porras and J.I. Cirac, Phys. Rev. Lett. **92**, 207901 (2004).
- [7] D. Porras and J.I. Cirac, Phys. Rev. Lett. **93**, 263602 (2004).
- [8] D. Leibfried *et al.*, Rev. Mod. Phys. **75**, 281 (2003).
- [9] D.M. Meekhof *et al.*, Phys. Rev. Lett. **76**, 1796 (1996).
- [10] G. Morigi and S. Fishman, Phys. Rev. Lett. **93**, 170602 (2004).
- [11] W.M. Itano *et al.*, Science **279**, 686 (1998); T.B. Mitchell *et al.*, Science **282**, 1290 (1998).
- [12] D. Porras and J. I. Cirac, Phys. Rev. Lett. **96**, 250501 (2006).
- [13] R. Bulla, N.-H. Tong and M. Vojta, Phys. Rev. Lett. **91**, 170601 (2003).
- [14] This problem is related to that of a Kondo impurity in a finite-size metal, see W.B. Thimm, J. Kroha, and J. von Delft, Phys. Rev. Lett. **82**, 2143 (1999).
- [15] H. Dekker, Phys. Rev. A **35**, 1436 (1987).
- [16] J. Wilkie, Phys. Rev. E **68**, 027701 (2003).
- [17] Bray, A.J. and M.A. Moore, Phys. Rev. Lett. **49**, 1545 (1982).
- [18] R. Egger and C.H. Mak, Phys. Rev. B **50**, 15210 (1994).
- [19] Y. Nakamura *et al.*, Phys. Rev. Lett. **88**, 047901 (2002).
- [20] Y. Makhlin and A. Shnirman, Phys. Rev. Lett. **92**, 178301 (2004).